Performance Evaluation of 802.16e in Vehicle to Vehicle Channels

Beibei Wang, Indranil Sen, David W. Matolak
School of Electrical Engineering & Computer Science
Ohio University
Athens, OH 45701
email: {bw221803, is809902, matolak} @ohiou.edu

Abstract— **Vehicle to Vehicle (V2V) communications have drawn much attention in the past few years. The IEEE 802.16e standard systems can be considered potential candidates for these applications due to their attractive features, like high data rate, mobility support, etc. In this paper, we evaluate the performance of an 802.16e system with the OFDMA air interface in two non-stationary vehicle to vehicle (V2V) channels: an open area high traffic density (OHT) channel and an urban (UOC) channel. We first introduce the non-stationary V2V channel models developed from empirical data. Then we provide a brief overview of 802.16e and introduce three channel estimation schemes that apply to different scenarios. Finally, we evaluate the performance of the 802.16e system over the proposed non-stationary V2V channel models. We show that the proposed channel estimation methods provide a good tradeoff between channel estimation accuracy and computational complexity. We also illustrate that system performance in non-stationary channels is more volatile than in stationary channels.**

Keywords-V2V channel, 802.16e, WMAN

I. INTRODUCTION

Vehicle-to-vehicle (V2V) communication systems will be an integral part of future intelligent transportation systems (ITSs) [1], and work on various aspects of ITSs [2] has been growing substantially in recent years. There is great potential for both commercial and non-commercial applications that can make use of V2V communication. Some of the obvious benefits for ITS are the ability to improve road safety, to make commuters aware of traffic conditions, and to enable faster processing at toll-booths. Additionally, independent consumer applications, such as transmission of multimedia content between different traveling cars, may become common.

A recent standard for V2V communication in the 5.9 GHz unlicensed national information infrastructure (UNII) band has been developed [1], aiming to enable support for high mobility platforms using the 802.11 protocol [8]. The other potential candidate in this standard is the IEEE 802.16e wireless metropolitan area network (WMAN) standard [7]. It is a newer, yet well-known high rate mobile air interface operating in the 2-6 GHz frequency range, which in addition to its high data rate, also provides scalable bandwidth, quality of service (QoS) support, and high spectral efficiency. The IEEE 802.16e standard allows two network topologies: point-to-multipoint (PMP) and mesh mode. In the former, data traffic only occurs between the subscriber station (SS) and the base station (BS), whereas in the latter, data traffic can occur directly between any two SSs and can be routed through multiple SSs. The mesh topology, together with the advanced multiple access scheme—orthogonal frequency division multiple access (OFDMA)—provides the robust network configuration required for the fast variations encountered in the vehicular environment in high mobility settings, making IEEE 802.16e a strong candidate for inter vehicle communication (IVC).

In this paper, we study the performance of 802.16e with different channel estimation methods in two V2V channels, a highway channel we term the open area high vehicle traffic density (OHT) channel and an urban channel. For consistency with prior work [5] where we measured and modeled the urban channel with both the antenna inside and outside the vehicle, we use the notation (UOC) for our urban channel, with the antenna outside the car. Since V2V communication system deployments are in their initial stages, understanding and accurately modeling the propagation environment is vital to design, performance prediction, and optimization of these systems. Several analytical and empirical models have been proposed to model the V2V channel under varying geographical and traffic conditions [3]]-[[5]. Our study here employs our empirical, statistically non-stationary models [5].

II. CHANNEL MODEL

A V2V communication system might encounter several different propagation environments that vary with traffic density and geography. In our channel modeling work [5] we have classified the V2V propagation channel into 5 regions: UOC, urban-antenna inside car (UIC), small city (S), open area–low traffic density (OLT), and OHT. The "open" areas are highways. Stochastic channel models for 5 and 10 MHz bandwidths for all these regions have been developed, using data collected in different cities and on several highways, at a carrier frequency of 5.12 GHz. This frequency is actually in an aeronautical band, specifically the microwave landing system (MLS) extension band, designated for use at large airports. Since the wavelengths in this MLS band and the unlicensed band at 5.2 GHz are very close, characteristics we measured in this band should be very close to those in the unlicensed band. For more discussion regarding the channel models, readers are referred to [5]. For the purpose of this paper, we consider our 10 MHz UOC and OHT models. The reasons for choosing the 10 MHz bandwidth are two-fold: first, most of

the systems proposed for V2V communications use relatively wide bandwidths (e.g., 10 MHz for the WLAN-based schemes); and second, public safety (PS) applications have allocated bands of 10 MHz in 4940-4990 MHz for V2V applications.

The propagation channel can be modeled as a time varying linear filter. Hence, the impulse response of the filter can be used to completely characterize the channel. The channel impulse response (CIR) is defined as the function $h(\tau;t)$, which represents the response of the channel at time t to an impulse input at time $t-\tau$. Mathematically, we have,

$$h(\tau;t)=\sum_{l=0}^{L-1} z_l(t)\alpha_l(t)e^{j\theta_l(t)}=\sum_{l=0}^{L-1} h_l(t)\delta[\tau-\tau_l(t)] \qquad (1)$$

where $\alpha_l(t)$ represents the l^{th} received amplitude, and the argument of the exponential term is the l^{th} received phase. The l^{th} multipath component has a time-varying delay $\tau_l(t)$, the δ-function is the Dirac delta. As compared to conventional representations of the CIR [6], we have employed an additional term in the CIR equation: the "persistence process" $z(t)$, used to account for the finite "lifetime" of propagation paths. V2V environments can have frequent and rapid channel changes due to mobility and low transmitting and receiving antenna heights. Thus for modeling, multipath components can be associated with a "birth/death" (i.e., on/off) process. For the tap persistence process, we employ the frequently used method of modeling an on/off process by a Markov chain. State 1 denotes the presence of multipath in a given delay bin and state 0 signifies the absence of multipath. We developed 1st-order 2-state Markov chains, specified by two matrices, the transition *(TS)* matrix and the steady-state *(SS)* vector, defined as follows,

$$TS=\begin{bmatrix} P_{00} & P_{01} \\ P_{10} & P_{11} \end{bmatrix}, \quad SS=\begin{bmatrix} P_0 \\ P_1 \end{bmatrix} \qquad (2)$$

Each element P_{ij} in matrix *TS* is defined as the probability of going from state i to state j, and each *SS* element P_j gives the "steady state probability" associated with the j^{th} state. The tap amplitude distributions for the empirical channel are modeled using the Weibull distribution. The Weibull model offers substantial flexibility, as it has two parameters,

$$p_W(x)=\left(\beta/a^{\beta}\right)x^{\beta-1}\exp\left(-(x/a)^{\beta}\right) \qquad (3)$$

where β is a shape factor that determines fading severity, $a=\sqrt{E(x^2)/\Gamma[(2/\beta)+1]}$ is a scale parameter, and Γ is the gamma function. A value of β=2 yields the well-known Rayleigh distribution, and β<2 implies more severe fading. Table 1 lists the channel model parameters for 10 MHz UOC channel. We also provide example correlation coefficients among the taps.

III. System Model

The OFDMA scheme provides flexibility in subcarrier allocation. In the IEEE 802.16e standard [7], two mandatory distributed permutation allocations for the OFDMA based air interface are available: the partial usage of subchannels (PUSC) and full usage of subchannels (FUSC). The distributed permutation reduces the probability of experiencing bad fading on all subcarriers of each subchannel. It functions as an interleaver with a large block size, thus enabling more coding gain than is attainable with contiguous subcarriers in each subchannel. The random permutation in subcarrier allocation also provides statistically identical channel qualities, thus fairness can be achieved among all active users. The standard also defines optional adaptive modulation and coding (AMC) permutations, which employ continuous sections in both time and frequency domains, providing vendors flexibility in choosing advanced scheduling algorithms. IEEE 802.16e has also provided several options for FFT size N for OFDMA based air interfaces: 128, 512, 1024, and 2024. Here we considering FFT size N=512, and some of the remaining key system parameters are in Table 2.

Table 1. Channel parameters for 10 MHz UOC region.

Tap Index k	Energy	β_k	$P_{00,k}$	$P_{11,k}$	P_1	$r_{k,2}$	$r_{k,3}$
1	0.8319	3.19	NA	1.0000	1.0000	0.6898	0.6518
2	0.0817	1.61	0.2717	0.9150	0.8956	1.0000	0.4922
3	0.0322	1.63	0.4401	0.8171	0.7538	0.4922	1.0000
4	0.0186	1.73	0.5571	0.7488	0.6382	0.5142	0.8479
5	0.0109	1.81	0.6955	0.6716	0.4813	0.5262	0.4608
6	0.0059	1.95	0.7843	0.5737	0.3362	0.5541	0.3986
7	0.0038	1.85	0.8693	0.5417	0.2218	0.7808	0.4838
8	0.0026	1.70	0.9136	0.5304	0.1553	0.4247	0.7468
9	0.0024	1.59	0.9322	0.4796	0.1156	0.7381	0.3924
10	0.0019	1.55	0.9436	0.4941	0.1003	0.6023	0.5346
11	0.0019	1.35	0.9549	0.5105	0.0843	0.8094	0.8106
12	0.0024	1.34	0.9655	0.5510	0.0714	0.5705	0.4102
13	0.0022	1.34	0.9707	0.5364	0.0594	0.6595	0.6172
14	0.0008	1.33	0.9772	0.5635	0.0495	0.4105	0.5672
15	0.0007	1.29	0.9778	0.5179	0.0440	0.7555	0.8850

Table 2: System Parameters

Channel Bandwidth (MHz)	*8.75*
Sampling Frequency f_{sam} (MHz)	*10*
FFT size	*512*
Basic OFDMA Symbol Period T_b (μs)	*51.2*
Cyclic Prefix Duration (μs)	*1.6*
OFDMA Symbol Period T_s (μs)	*52.8*

IEEE 802.16e has defined different subcarrier permutations for the uplink and downlink. In this paper we are focus on the uplink PUSC, in which each subchannel is composed of six tiles chosen by the random permutation, and each active user is assigned one or more subchannels. For the uplink PUSC with FFT size of 512, the leftmost 52 subcarriers and the rightmost 51 subcarriers are guard subcarriers. With the central DC subcarriers excluded, we have 408 subcarriers for data and pilot transmission. A typical system structure is illustrated in Figure 1.

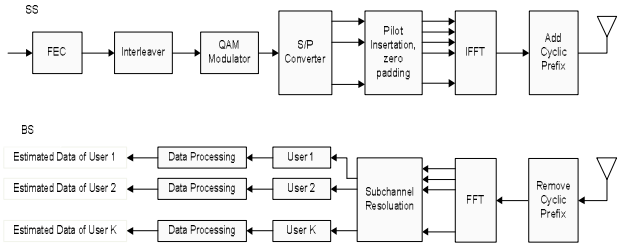

Figure 1: System Structure

The input data is passed through the convolution encoder, block interleaver, and the quadrature amplitude modulator (QAM) in sequence. The serialized QAM symbols are then converted to parallel data streams on assigned data subcarriers, and extra known pilot symbols are added onto the corresponding pilot subcarriers for estimation and detection purposes. After the inverse fast Fourier transform (IFFT), the resultant signal of the *k*th user can be written as

$$x_{kn}(i) = \sum_{m=-256}^{255} X_{kn}(m) e^{j2\pi im/N}, i = 0,1,....,N-1 \quad (4)$$

Where $x_{kn}(i)$ is the transmitted signal of the *k*th user on the *i*th sample of the *n*th OFDMA symbol, and $X_{kn}(m)$ is the transmitted symbol of the *k*th user on the *m*th subcarrier at the *n*th OFDMA symbol index, which can be expressed by

$$X_{kn}(m) = \begin{cases} d_{kn}(m), m \in I_{dk} \\ p_{kn}(m), m \in I_{pk} \end{cases} \quad (5)$$

where I_{dk} and I_{pk} are the index sets of data subcarriers and pilot subcarriers of the *k*th user, respectively. Note that subcarriers are not allowed to be shared among users. After the IFFT, a cyclic prefix longer than the maximum delay spread of the channel is then inserted into $x_{kn}(t)$ to avoid the interference caused by multipath. Here we assume all active users in the system are perfectly synchronized with the BS. With $\tau = l/f_{sam}$ in the channel model (1), the received signal at the *i*th sample for the *n*th symbol is

$$y_n(i) = \sum_{k=1}^{K} \sum_{l=0}^{L-1} h_{kn}(l) x_{kn}(i-l) + w_n(i) \quad (6)$$

where *K* is the number of active users and $w_n(i)$ is an additive white Gaussian noise (AWGN) sample.

On the receiver side, Figure 2, first the cyclic prefix is removed, and an FFT is then performed to demodulate the received signal

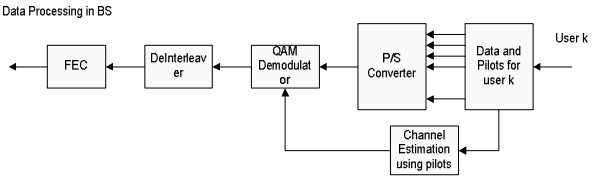

Figure 2: Data Processing Block in BS

The post-FFT signal is

$$Y_n(m) = X_{kn}(m) H_{kn}(m) + W_n(m) \quad (7)$$

where $W_n(m)$ is the complex Gaussian noise with variance N_0, and $H_{kn}(m)$ is the channel frequency response of user *k* on subcarrier *m* during the *n*th OFDMA symbol, which can be expressed by

$$H_{kn}(m) = \sum_{l=0}^{L-1} h_{kn}(l) e^{j2\pi lm/N} \quad (8)$$

We use $\hat{H}_{kn}(m)$ to represent our estimate of channel fading coefficient $H_{kn}(m)$, then the estimated transmitted QAM symbol of the *k*th user on the *m*th subcarrier for the *n*th OFDMA symbol is the element in the QAM constellation with the minimum Euclidean distance to the channel-equalized symbol $\hat{Y}_n(m) = Y_n(m) / \hat{H}_{k,n}(m)$:

$$\hat{X}_{kn}(m) = \min_{0<q<M} | S_q - \hat{Y}_n(m) | \quad (9)$$

with S_q the *q*th element in our QAM constellation, and $M=16$ is the QAM constellation size. The demodulated data is then passed through the deinterleaver and decoder.

With the uplink PUSC allocation, each subchannel consists of six tiles chosen by random permutation. The positions of pilots and data symbols are shown in the tile structure in Figure 3.

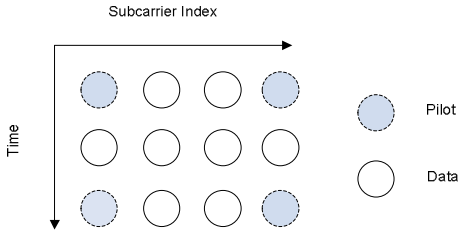

Figure 3: Tile Structure

.

There are multiple channel estimation (CE) algorithms in the literature. The optimum algorithm is a 2-D Wiener filter, but it is computationally expensive. Sub-optimum estimation schemes have lower computational complexity by separating the time and frequency-domain estimation algorithms. We propose three simplified CE methods using averages and linear interpolation techniques to allow

tradeoffs between channel estimation accuracy and computational complexity.

i) CE 1 uses the average of the pilots in both time and frequency domains to obtain the channel estimates. CE 1 applies to the case where the channel coherence time is much larger than the tile duration, so the channel response on the three OFDMA symbols within a tile can be approximated as constant; CE 1 also requires that channel fading varies little over the four adjacent subcarriers in the same tile.

ii) CE 2 uses the average of the pilots in the time domain and linear interpolation in the frequency domain to estimate the channel fading on the data subcarriers. Like CE 1, CE 2 applies to the case where the channel coherence time is much larger than the tile duration, thus the channel response on the three OFDMA symbol durations can be approximated as constant. Different from CE 1 though, in the frequency domain CE 2 assumes that fading amplitude and phase over four adjacent subcarriers in a tile structure is approximately linear.

iii) CE 3 uses linear interpolation of the pilots in both time and frequency domains to obtain the channel fading estimates on data subcarriers. In the time domain, CE 3 applies to the case where the channel response over three OFDMA symbol durations in the tile is well modeled as linear. Similar to CE 2, CE3 assumes that the channel response in the frequency domain over four adjacent subcarriers in a tile is linear.

Assuming the average fading energy on each subcarrier is 1, we use the mean-square error to quantify the accuracy of our different CE methods

$$MSE = \sum_{k=1}^{K} \sum_{n=1}^{N_s} \sum_{m \in I_k} \frac{1}{K N_s N_{kused}} | H_{kn}(m) - \hat{H}_{kn}(m) |^2 \quad (10)$$

where N_s is the number of transmitted OFDMA symbols, I_k is the kth user subcarrier set, and N_{kused} is the number of subcarriers in I_k. In the following section, we will evaluate the performance of the OFDMA based WMAN in our V2V channel models described in Section II using the three different channel estimation methods, and compare their performance with that of the perfect channel estimation case.

IV. Simulation Results

All our simulations in this section use the uplink PUSC permutation in the frequency domain and random subchannel scheduling in the time domain. Modulation is 16-QAM and unit average fading energy is assumed on each subcarrier. All simulations were conducted in Matlab®, using the system parameters shown in Table 1. For simplicity, we only investigate system performance with/without the mandatory convolutional code of rate r=1/2, constraint length 7 (memory 6, with generator vectors $\mathbf{g_1}=(171)_8$, $\mathbf{g_2}=(133)_8$). Hard decision Viterbi decoding is performed using Matlab's built-in convolutional encoding/decoding routines. Interleaving is performed according to the specification in the 802.16e standard.

Figure 4 plots BER performance versus E_b/N_0 for the OHT V2V channel. The BER was obtained by averaging over 5 simulation runs with N_b=14.2 million transmitted bits in each run. A Doppler frequency of f_D=458 Hz, which corresponds to a speed of v=60miles/hour with a carrier frequency of f_c=5.15 GHz, was used. It is shown that in the OHT channel, CE 1 has a small performance gain over CE 2 and CE 3 in the coded case. The performance gain of perfect channel estimation (PE) over CE 1 is approximately 1.6 dB for the case without coding, and 1.2 dB for the case with coding. The small gain illustrates that CE 1 provides a good tradeoff between computational complexity and performance.

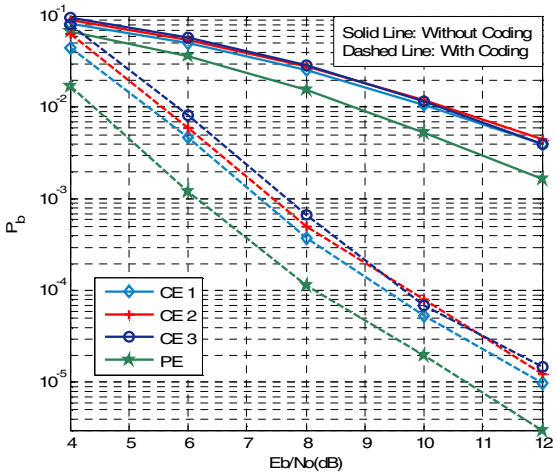

Figure 4: BER vs E_b/N_0 for OHT V2Vchannel, N=512, uplink PUSC, active user number K=5, f_D=458 Hz.

Figure 5 depicts BER performance versus E_b/N_0 for the UOC V2V channel. Similar to the OHT case, the BER is obtained by averaging over 5 simulation runs with N_b=14.2 million transmitted bits in each run.

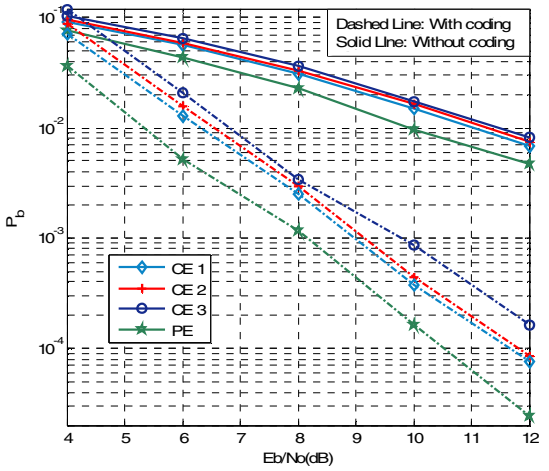

Figure 5: BER vs E_b/N_0 for UOC V2Vchannel, N=512, uplink PUSC, active user number K=5, f_D=286 Hz.

The Doppler frequency here is f_D=256 Hz, which corresponds to a typical speed of v=36 miles/hour in an urban area. Compared with the OHT case where the first tap has more than 93% of the total energy and a Weibull parameter of 4.3, the performance in the UOC case, where the first tap has 83% of the total energy with a Weibull parameter of 3.16, is noticeably worse. Again, it is shown that CE 1 has slightly better performance than CE 2 and CE 3, and the performance gain of PE over CE 1 is 1.2 dB for the case without coding, and 1 dB for the case with coding. Figure 6 illustrates the BER performance versus different runs for the OHT and UOC channels, with several values of

E_b/N_0. The number of transmitted bits for each run is N_b=14.2 million. Due to the non-stationary characteristics of the channel, we get different performance for different runs even though we are counting more than 500 errors for each run; this is not usually seen in stationary channel models. Running more bits per run can reduce this variation of course, but the non-stationary channel still requires a large number of error counts, i.e., a long transmission duration, to yield a stable performance estimate. Figure 7 shows channel estimation MSE for our three different estimation methods versus Doppler frequency for the OHT and UOC channels. Only the higher end of the Doppler frequency range is considered for OHT case since it is highway channel. From this figure, we can see that when Doppler frequency increases, the MSE of CE 1 and CE 2, which are based on the assumption that fading varies little on the three OFDMA symbols within each tile, degrades due to the increasing channel variation in the time domain. In contrast, for CE 3, which is based on linear interpolation in both time and frequency domains, its MSE is not a strong function of Doppler frequency. It is also observed that CE 1 and CE 2 perform better than CE 3 at lower Doppler frequencies for both OHT and UOC, and performs worse than CE 3 at higher Doppler frequency (>600) for the UOC case.

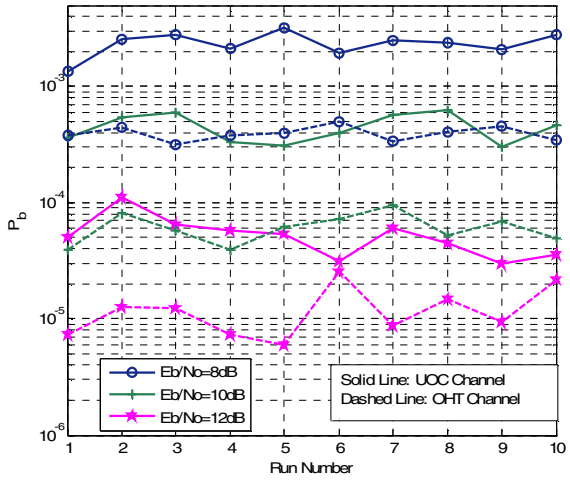

Figure 6: BER vs different runs for OHT and UOC channel, N=512, uplink PUSC, active user number K=5, f_D=458 Hz for OHT channel, and 286 Hz for UOC channel.

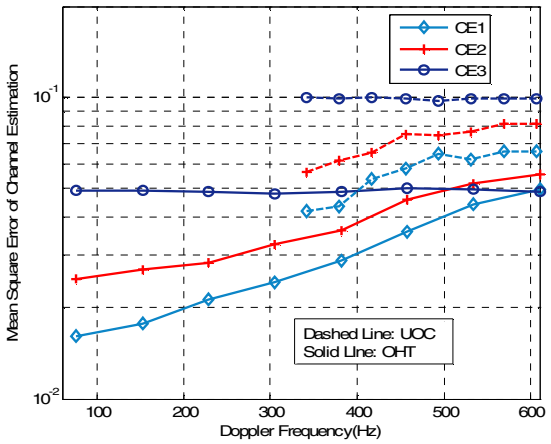

Figure 7: MSE vs Doppler frequency for OHT and UOC channel respectively, N=512, uplink PUSC, active user number K=5.

V. SUMMARY AND CONCLUSION

In this paper, we evaluated the performance of an OFDMA based WMAN transmission scheme in two non stationary vehicle to vehicle (V2V) channels: one was the open, high-vehicle traffic density channel (OHT), the other was the urban channel (UOC). We first introduced the non-stationary V2V channel models we have developed. Then we gave a brief overview of 802.16e, illustrated the system structure, described the OFDMA signal, and introduced three channel estimation methods that apply to different scenarios. Finally, we simulated the performance of the 802.16e system over the proposed non-stationary V2V channel models. It has been shown that the proposed channel estimation methods provide good tradeoffs between channel estimation accuracy and computational complexity in the non-stationary channels. It was also shown that the 802.6e system performance in the non-stationary channel is more volatile than that in stationary channels.

References

[1] ASTM E2213, " Standard Specification for Telecommunications and Information Exchange Between Roadside and Vehicle Systems – 5GHz Band Dedicated Short Range Communications (DSRC) Medium Access Control (MAC) and Physical Layer (PHY) Specifications, http://www.astm.org, February 2007.

[2] ITS project website, http://www.its.dot.gov/index.htm, February 2007.

[3] C. S. Patel, G. L. Stuber, T. G. Pratt, "Simulation of Rayleigh Faded Mobile-to-Mobile Communication Channels," *Proc. IEEE Veh. Tech. Conf.*, vol. 1, pp. 163-167, October 2003.

[4] J. Maurer, T. Fugen, T. Schafer, W. Wiesbeck, "A New Inter-Vehicle Communications (IVC) Channel Model," *Proc. IEEE Veh. Tech. Conf.*, vol. 1, pp. 9-13, September 2004.

[5] D. W. Matolak, I. Sen, W. Xiong, "Channel Modeling for V2V Communications," *Proc. Vehicle-to-Vehicle Communications workshop (V2VCOM 2006)*, San Jose, CA, July 21, 2006.

[6] G. Stuber, *Principles of Mobile Communications*, Kluwer Academic Publishers, Norwell, MA, 1996.

[7] IEEE 802.16e™: Air Interface for Fixed and MobileBroadband Wireless Access, Std. Systems, 2005.

[8] IEEE, Std. 802.11: Wireless LAN Medium Access Control (MAC) and Physical layer (PHY) Specifications, 1999.